Journal of ELECTRONIC MATERIALS, Vol. 47, No. 2, 2018
DOI: 10.1007/s11664-017-5824-y

TOPICAL COLLECTION: 59TH ELECTRONIC MATERIALS CONFERENCE 2017

Photoelectrochemical Water Oxidation by GaAs Nanowire Arrays Protected with Atomic Layer Deposited NiO_x Electrocatalysts

JOY ZENG,[1] XIAOQING XU,[2,3] VIJAY PARAMESHWARAN,[4] JON BAKER,[1] STACEY BENT,[1] H.-S. PHILIP WONG,[2] and BRUCE CLEMENS[5,6]

1.—Chemical Engineering Department, Stanford University, Stanford, CA, USA. 2.—Electrical Engineering Department, Stanford University, Stanford, CA, USA. 3.—Stanford Nanofabrication Facility, Stanford University, Stanford, CA, USA. 4.—US Army Research Laboratory, Adelphi, MD, USA. 5.—Materials Science and Engineering Department, Stanford University, Stanford, CA, USA. 6.—e-mail: bmc@stanford.edu

Photoelectrochemical (PEC) hydrogen production makes possible the direct conversion of solar energy into chemical fuel. In this work, PEC photoanodes consisting of GaAs nanowire (NW) arrays were fabricated, characterized, and then demonstrated for the oxygen evolution reaction (OER). Uniform and periodic GaAs nanowire arrays were grown on a heavily *n*-doped GaAs substrates by metal–organic chemical vapor deposition selective area growth. The nanowire arrays were characterized using cyclic voltammetry and impedance spectroscopy in a non-aqueous electrochemical system using ferrocene/ferrocenium (Fc/Fc+) as a redox couple, and a maximum oxidation photocurrent of 11.1 mA/cm^2 was measured. GaAs NW arrays with a 36 nm layer of nickel oxide (NiO_x) synthesized by atomic layer deposition were then used as photoanodes to drive the OER. In addition to acting as an electrocatalyst, the NiO_x layer served to protect the GaAs NWs from oxidative corrosion. Using this strategy, GaAs NW photoanodes were successfully used for the oxygen evolution reaction. This is the first demonstration of GaAs NW arrays for effective OER, and the fabrication and protection strategy developed in this work can be extended to study any other nanostructured semiconductor materials systems for electrochemical solar energy conversion.

Key words: Oxygen evolution reaction, water oxidation, GaAs nanowire, atomic layer deposition, nickel oxide, corrosion protection

INTRODUCTION

Solar flux is the largest potential source of renewable energy,[1] and photoelectrochemical (PEC) cells are a promising option for directly converting solar energy into chemical fuels such as hydrogen and higher-order hydrocarbons including methanol and ethylene. In the simplest version of these devices, energy from photons is used to generate hydrogen and oxygen from water via the following half reactions[2]:

$$4H^+ + 4e^- \rightarrow 2H_2 \quad \text{(HER)}$$
$$2H_2O \rightarrow O_2 + 4H^+ + 4e^- \quad \text{(OER)} \quad (E = 1.23\ \text{eV})$$

Tandem PEC devices integrate light absorption and electrochemical conversion into a single step, and are attractive over other non-integrated architectures such photovoltaic-electrolysis devices[3] because they can form simpler systems that have lower installation and material costs. In a tandem PEC device, a semiconductor photoanode is coupled

(Received July 10, 2017; accepted September 19, 2017; published online October 12, 2017)
Joy Zeng, Xiaoqing Xu and Vijay Parameshwaran have contributed equally to this work.

to a corresponding photocathode that typically has a different bandgap energy. Water oxidation, or the oxygen evolution reaction (OER), occurs at the photoanode surface while hydrogen reduction, or the hydrogen evolution reaction (HER), occurs at the photocathode surface.[4] Requirements for these electrode materials include proper band edge alignment with HER and OER potentials, stability in HER or OER conditions, efficient charge transport, low kinetic overpotentials achieved with catalytically active surfaces, and low cost.[5]

On the photoanode side, a major challenge is that the OER is an oxidation reaction, and finding high-performing materials that are stable in corrosive oxidation conditions is difficult. Many materials such as silicon (Si) and gallium arsenide (GaAs) that have bandgap energies, crystal quality, and light absorption properties well suited for solar conversion applications are not chemically stable in OER conditions. Metal oxides are stable in OER conditions, but their inefficient light absorption due to wide and indirect bandgap energies, and a tendency to have poor charge transport properties, have limited their photoanode performance.[6] One strategy to address this challenge has been to use thin layers of protective coatings to stabilize materials that would otherwise corrode under operation, and a variety of metal oxides including TiO_2, SiO_2, MnO_x, and NiO_x have been investigated for this purpose.[7–9]

Herein, we report the use of a GaAs nanowire (NW) array coated with an atomic layer deposited, iron-doped, nickel oxide (NiO_x) layer as a photoanode for stable, solar-driven water oxidation. GaAs is a III–V semiconductor that is known to be a high efficiency solar conversion material due to its good crystalline quality, high carrier mobility, and direct bandgap.[10,11] Furthermore, the bandgap energy of GaAs, 1.42 eV, is near the ideal solar absorption bandgap from the Shockley–Queisser limit.[12] Semiconductors grown as nanowire arrays are attractive for PEC applications because nanowires have (1) improved light absorption due to optical scattering and trapping effects, (2) improved charge transport due to orthogonalization of light absorption length with carrier diffusion length, and (3) a large surface area to perform electrochemical reactions that allow for better catalyst loading and reduced electron surface flux that reduces kinetic requirements on catalyst materials.[2,6] Recently, Hu et al.[13] performed optical, electronic, and non-aqueous electrochemical characterizations on n-doped GaAs NW arrays, reporting inherent energy conversion efficiencies of $\sim 8.1\%$ along with high optical absorption and minimal reflection.

However, GaAs itself is not stable in aqueous photoanodic conditions, and to our knowledge, the use of GaAs NW arrays as photoanodes to drive water oxidation has not been reported. Therefore, in this work, nickel oxide, deposited via atomic layer deposition (ALD), was used as a protection layer for a GaAs NW array. Ni-Fe oxides have been shown to have good catalytic activity for the OER, and ALD deposited nickel oxides are known to be smooth, dense films that, when put in alkaline conditions, form an electrocatalytically active outer layer that contains $Ni(OH)_2$, NiOOH, and trace amounts of iron. The iron is often incorporated from the electrolyte, and Ni(Fe)OOH has been shown to be essential for the high catalytic activity of nickel oxide (NiO_x) films.[14,15] In this work, the NiO_x layer functions to both protect the GaAs NWs from corrosion and to act as a catalyst for the OER reaction. Similar strategies that take advantage of both the protective and catalytic effects of conformally coated NiO_x catalysts, deposited via reactive sputtering, have been reported on photoanode materials including planar silicon[16,17] and *n*-CdTe.[17] However, ALD offers the ability to achieve highly uniform protective layers over non-planar surface features such as nanowires and is a more benign depositing process as compared to reactive sputtering. Here, we demonstrate the use of an ALD-deposited metal oxide to protect a semiconductor nanowire array.

EXPERIMENTAL METHODS

Sample Preparation

GaAs NW arrays were grown using metal–organic chemical vapor deposition (MOCVD) selective area growth through patterned SiO_2 masks. The masks were patterned using E-beam lithography to define arrays of nano-holes. Planar GaAs substrate and GaAs substrate coated with SiO_2 were also prepared then used for comparison in photocurrent measurements.

NiO_x films were deposited using a custom built ALD reactor, in which nickelocene ($NiCp_2$) and ozone were used as the precursors, and N_2 as the carrier gas. Film thicknesses were then characterized using spectroscopic ellipsometry. Trace amounts of iron were incorporated into the NiO_x films later, via the electrolyte, during aqueous electrochemical measurement. The electrolyte was intentionally saturated with iron to enhance iron incorporation into the film, but the samples were not explicitly "preconditioned"[15] to enhance iron incorporation. Additional details can be found in the supplemental information.

Samples were then built into electrodes to be used for electrochemical characterization. This was done by soldering a wire to the back of the sample using indium and then applying Apiezon Black Wax W around the back and sides of the sample to define an active area. A representative sample electrode can be seen in Supplemental Fig. S1.

Electrochemical Characterization

Both non-aqueous and aqueous measurements were performed in a 3-electrode cell setup, with the sample as the working electrode. For non-aqueous measurements, the electrolyte was 0.002 M ferrocene (98%, Sigma Aldrich)/0.002 M ferrocenium tetrafluoroborate (technical grade, Sigma Aldrich)/ 0.1 M ammonium chloride (99.5%, Sigma-Aldrich) in anhydrous methanol. For aqueous measurements, the electrolyte was 0.1 M potassium hydroxide (> 85%, Sigma Aldrich) in DI water, purged with N_2 gas. As mentioned earlier, the 0.1 M KOH solution was also intentionally saturated with iron via addition of $Fe(NO_3)_3$. Illumination was generated using a Newport Class 3A solar simulator lamp calibrated to 1 sun (100 mW/cm^2). For current–voltage curves, photocurrent density was determined by measuring photocurrent generated by samples exposed to chopped light, subtracting dark-generated current from light-generated current, and normalizing by geometric area. Electrochemical impedance (EIS) measurements were taken in the absence of illumination, in contact with the non-aqueous electrolyte, in a frequency range of 500 kHz to 1 Hz, and capacitance (C) was extracted from the measurements using Randle's equivalent circuit model (see supplemental information for details). The area used to normalize the photocurrent and the capacitance was the physical area of the samples exposed in electrolyte, and was obtained from the as-fabricated electrodes by using ImageJ software with a ruler for scale.

RESULTS AND DISCUSSION

Non-aqueous Electrochemistry

Non-aqueous photoelectrochemical (PEC) characterization of the GaAs NW arrays using the ferrocenium/ferrocene (Fc/Fc+) redox couple in anhydrous methanol was initially used to probe the photoelectrochemical properties of the GaAs NWs. This was done prior to NiO_x deposition to study the intrinsic PEC properties of the NWs themselves. The non-aqueous electrolyte helped to minimize sample oxidation, and the Fc/Fc+ redox couple is kinetically facile and reversible, which ensured that electron transfer kinetics from the semiconductor to the electrolyte would not be not rate-determining. Figure 1 shows an SEM image of a NW array that was measured. The sample has a NW pitch size of 550 nm and a NW diameter of 110 nm, with a NW length of 775 nm.

The NW-patterned sample had several orders of magnitude enhancement of photocurrent density over the planar substrate samples. Current–voltage curves from non-aqueous electrochemical measurements can be seen in Fig. 2. The maximum photocurrent density for a bare n+ GaAs substrate (with a manufacturer-specified carrier concentration of 1.56–3.92 $\times$ 10^{18} cm^{-3}) was 0.12 mA/cm^2, and for a n+ GaAs substrate coated with SiO_2, was 0.01 mA/cm^2. The sample containing the NW array had a much higher photocurrent density of 9.97 mA/cm^2. The SiO_2-coated substrate displayed almost no photocurrent because the presence of the SiO_2 layer inhibited charge transport across the electrode/electrolyte interface.

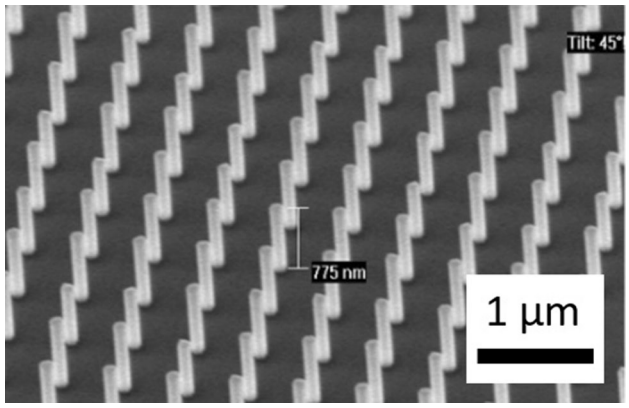

Fig. 1. SEM image of a GaAs NW array. The image was taken using a 45° tilted sample holder. The periodic GaAs NW array was grown on n+ GaAs substrates through a nano-patterned SiO_2 mask. The NWs have a length of 775 nm, a diameter of 110 nm, and a pitch of 550 nm.

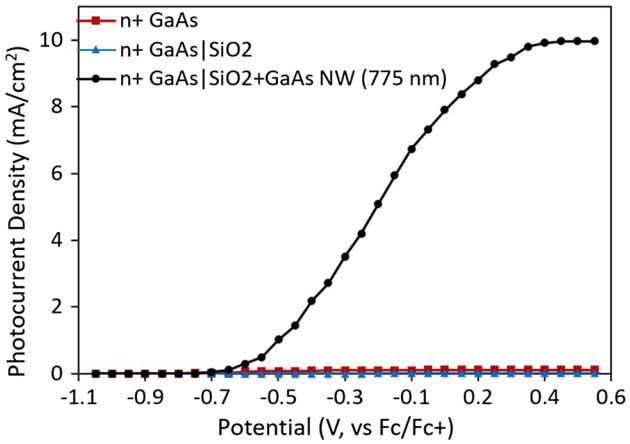

Fig. 2. Non-aqueous photocurrent measurements. Current density–voltage curves prior to NiO_x deposition are shown for a bare n+ GaAs substrate (red squares), n+ GaAs substrate uniformly coated with SiO_2 (blue triangles), and undoped 775 nm long GaAs NWs grown on an n+ GaAs substrate through a nano-patterned SiO_2 mask (black circles) (Color figure online).

The photocurrent generated by GaAs NW arrays reported here is less than that reported by Hu et al.[13] in non-aqueous electrochemistry for similar n-doped GaAs NW arrays (24.6 mA/cm^2) with a NW diameter of 135 nm, a length of 3 μm and a of 600 nm. However, this may be explained by the fact that the NWs reported by Hu et al. were much longer (3 μm) than the nanowires reported here. The photocurrent per total nanowire volume reported here is about twice that reported by Hu et al. Although light absorption through a material

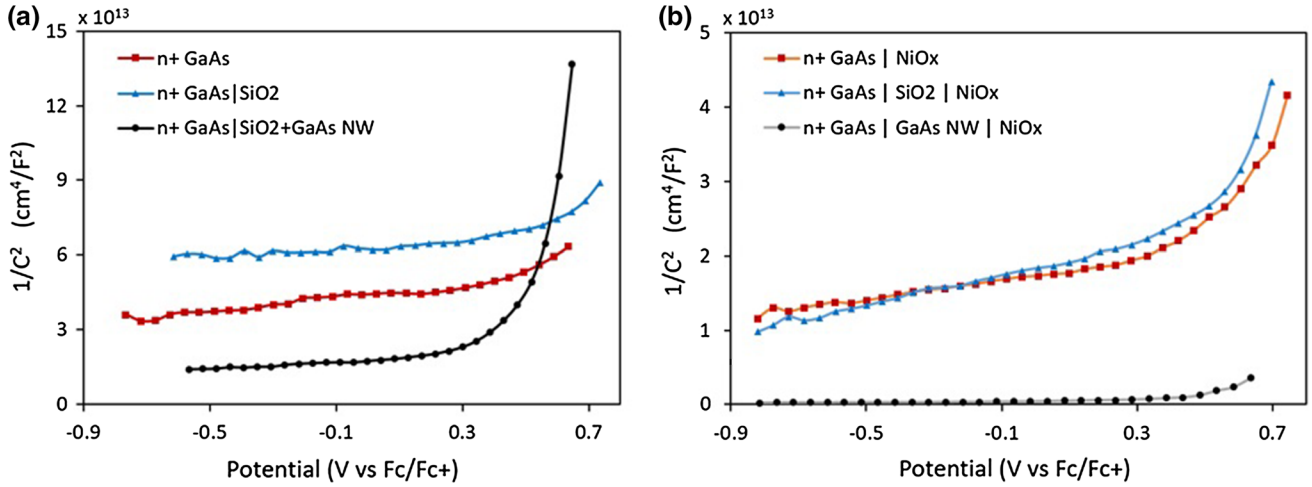

Fig. 3. Non-aqueous impedance measurements: Mott–Schottky plot of n+ GaAs substrate (red squares; 1.56–3.92 × 10^{18} cm^{-3}), n+ GaAs substrate uniformly coated with SiO_2 (blue triangles), and undoped 775 nm GaAs NWs grown on an n+ GaAs substrate through a nano-patterned SiO_2 mask (black circles) both prior to (a) and after (b) uniform 12 nm NiO_x coating. Measurements were taken in the absence of illumination, in contact with the ferrocene/ferrocenium redox couple, in a frequency range of 500 kHz to 1 Hz (Color figure online).

is not linear and experimental conditions may vary and contribute to the difference, with NW length taken into consideration, the photocurrent number reported here both reasonably agrees with what has been previously reported and demonstrates the high quality of our GaAs NWs.

EIS measurements were also taken to study NW-electrolyte junction. Graphs of $1/C^2$ versus V can be seen in Fig. 3, for samples both before and after NiO_x deposition. In both cases, there are two distinct, linear regimes. The regime below $\sim$ 0.3 V corresponds to samples in depletion, and the regime above $\sim$ 0.3 V corresponds to samples in accumulation. The NWs studied here were large enough to show a contribution to the EIS measurements, which can be seen with the distinctly different Mott–Schotty curves shown in Fig. 3 for the NW sample as compared to planar substrate samples. However, it is notable that the EIS measurements on the NW array samples reflect both depletion phenomena occurring in the NW array and in the underlying substrate, the specific contributions of which are difficult to elucidate. However, using the slope of the depletion regime for the substrate in Fig. 3a and the Mott–Schottky equation (see SI), we calculated a substrate doping density in the range of 0.93–1.48 × 10^{18} cm^{-3}, which was in reasonable agreement with the manufacturer's provided number of 1.56–3.92 × 10^{18} cm^{-3}. Additionally, though ALD deposited NiO_x is thought to be p type in nature,[18] the positive slopes of graphs in Fig. 3b indicate a dominant n type character of the samples, suggesting that the underlying n type GaAs substrate and the NWs made larger contributions to the EIS measurement than did the NiO_x layer. This may be because the thin NiO_x layer may have depleted quickly compared to the rest of the sample or because ALD oxides are typically polycrystalline or amorphous, so there may have been defect states that overshadowed the natural p type nature of the NiO_x.

Water Oxidation Using a NiO_x-Coated GaAs Nanowire Array

For a demonstration of water oxidation, two separate GaAs NW arrays were coated in NiO_x layers of 12 nm and 36 nm, respectively. SEM images of the two arrays prior to NiO_x coating can be found in Supplemental Fig. S3. Both arrays were then used to drive water oxidation over several potential sweep cycles and examined under SEM after electrochemical testing. As can be seen in Fig. 4a, the NW array coated in 12 nm NiO_x displayed failure features in the form of cracks along the NW array surface. It is likely that at some point, the electrolyte penetrated through the NiO_x layer and etched some of the GaAs substrate, leading to the cracked structures that were observed. However, it is notable that for a planar GaAs substrate that was also coated in 12 nm NiO_x and tested in the same conditions, no such failure features were observed. This indicates that NWs need thicker metal oxide protective layers than planar substrates do to achieve the same level of corrosion protection due to the special geometry. It is possible that this is because the NiO_x depositing may not have been perfectly conformal around the NWs, which caused them to be more susceptible to degradation. Additionally, with a NW geometry, there are surface features such as edges that would not be present in a planar sample and might be more difficult to protect with a metal oxide layer.

With a thicker, 36 nm NiO_x coating, no such failure features were observed, indicating successful protection of the NW surface using a thicker protective layer. For this sample, the active area

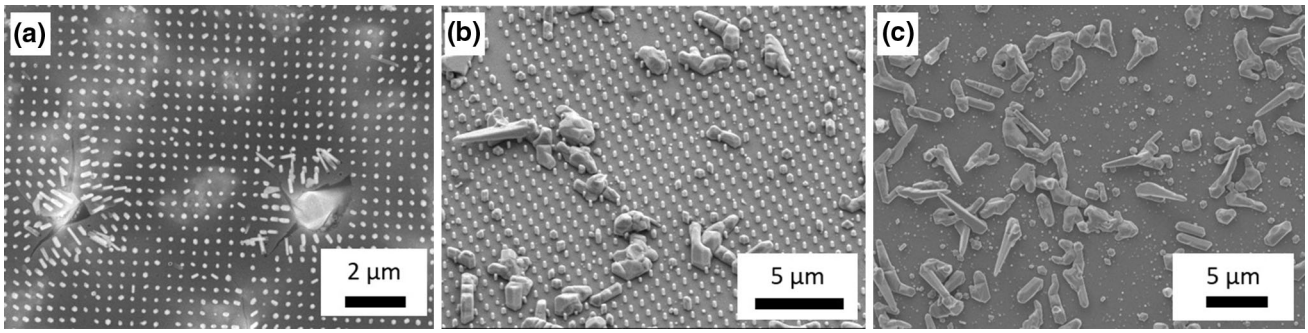

Fig. 4. SEM images of NiO_x coated GaAs NW arrays after OER measurements. (a) Plan view of representative failure features seen on a NW array that was coated with a 12 nm NiO_x layer. (b, c) Different locations on the same sample that was coated with a 36 nm NiO_x layer. (b) This is a section within the NW array, taken at a 30° tilt, and (c) is a plan view of a section of exposed substrate. Random nanostructures visible in both (b, c) are extra GaAs growths on the SiO_2 template due to non-ideal growth conditions. Notably, no cracks were observed post-measurement for the thicker protection layer.

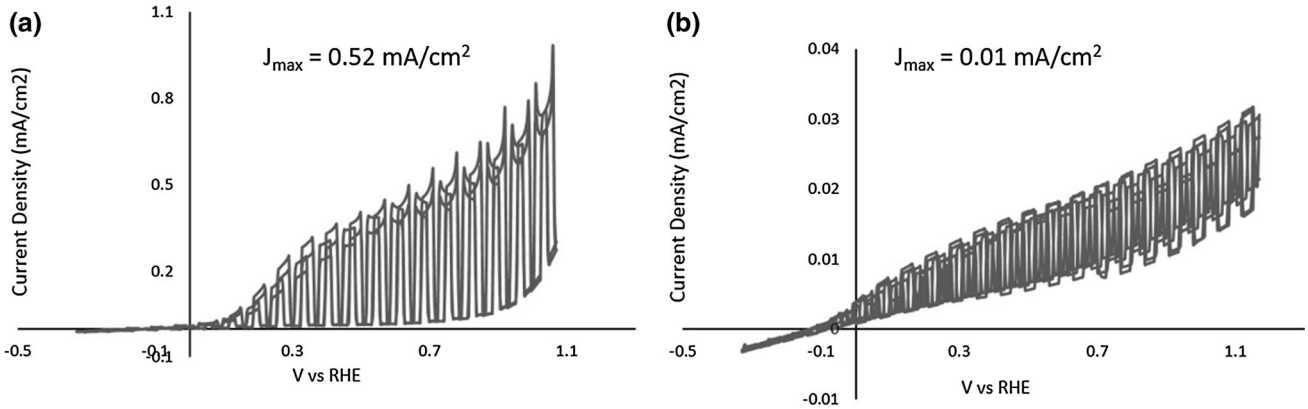

Fig. 5. Water oxidation using a NiO_x coated GaAs NW array and GaAs substrates. (a) 36 nm NiO_x on a small GaAs NW array; the active area of this sample included both unpatterned substrate and a small NW array (that was $<$ 2% of the total active area). (b) 36 nm NiO_x on bare GaAs substrate. All samples were measured in 0.1 M KOH and exposed to chopped 1 sun illumination.

included both the NW array (Fig. 4b) and an unpatterned part of the sample (Fig. 4c). The random nanostructures that can be seen in both Fig. 4b and c are extra GaAs deposits on the SiO_2 template due to non-ideal growth conditions. The growth conditions can be further optimized to prevent this undesired deposit on the SiO_2 template.

The NW-patterned sample coated with 36 nm NiO_x had enhanced photocurrent over a corresponding NiO_x-coated GaAs substrate. Current–voltage curves from water oxidation measurements can be seen in Fig. 5. The NW-patterned sample generated a photocurrent density of 0.52 mA/cm^2 and the GaAs substrate generated 0.01 mA/cm^2. The photocurrent reported for the NW array sample is smaller than expected because the reported photocurrent density was for an entire sample area, in which the NW array accounted for only less than 2% of the total active area. Resistance from the NiO_x film probably also contributed to some amount of performance loss, which may help explain the low photocurrent seen for the n+ GaAs substrate. However, previous reports suggest that in the thickness range reported here, NiO_x films tend to have high conductivities and relatively thickness-independent performance.[15,17] A future step beyond this exploratory study could be to further describe or quantify resistive losses from the NiO_x film. From these results, we qualitatively showed that with a sufficiently thick protection layer, an ALD NiO_x-protected GaAs NW photoanode could successfully be used to drive water oxidation.

CONCLUSIONS

In this work we report various electrochemical characterizations, both non-aqueous and aqueous, of GaAs NW arrays. Non-aqueous electrochemical characterization yielded photocurrent density numbers in good agreement with previous reports. Extending past non-aqueous measurements, GaAs NW arrays were then coated in protective and electrocatalytically active nickel oxide layers via ALD and then used to drive the water oxidation reaction. Our results qualitatively showed that NW-structured surfaces required thicker protective coatings than planar substrates did, but that with

a sufficiently thick protective coating, it was possible to achieve water oxidation using a GaAs NW-based photoanode, while not causing any corrosion to the NWs. This the first demonstration of GaAs NW arrays for effective OER, to the best of our knowledge. Further studies to quantify the amount of photocurrent that can be generated from such material systems, as well as studies to assess long-term cycling stability, are natural next steps to extend this work.

GaAs NWs are intrinsically interesting materials to study for PEC applications, and this work is an important step in realizing their application in water-splitting photoanodes. Though the results displayed here are qualitative, they are promising and suggest that further optimization of NW dimensions and growth conditions, as well as NiO_x thickness, could lead to a high-performance photoanode. Additional future work can also be used to further probe and understand processes that occur at interfaces between semiconductor, protective catalyst, and electrolyte for similar material design motifs. Though there are a fair number of reports on metal oxide protective layers for planar electrodes, the same strategy on nanostructured surfaces, enabled by ALD, is not as well-studied. We hope that future work can lead to more general design principles for nanostructured, metal oxide protected photoanodes, which may help enable further development of tandem PEC technologies.

ACKNOWLEDGEMENTS

This work was supported in part by the member companies of the Stanford Initiative for Nanoscale Materials and Processes (INMP). This work was also supported as a part of the Center for Nanostructuring for Efficient Energy Conversion (CNEEC) at Stanford University, an Energy Frontier Research Center funded by the U.S. Department of Energy, Office of Basic Energy Sciences, under Award DE-SC0001060. Additional support comes from the Precourt Institute of Energy and the Bay Area Photovoltaic Consortium. H.S.P.W. was supported in part by the *Willard R. and Inez Kerr Bell Professorship* in the School of Engineering at Stanford University. The NW array growth was performed at the MOCVD lab of the Stanford Nanofabrication Facility (SNF).

ELECTRONIC SUPPLEMENTARY MATERIAL

The online version of this article (doi: 10.1007/s11664-017-5824-y) contains supplementary material, which is available to authorized users.

REFERENCES

1. W. Hermann, *Energy* 31, 12 (2006).
2. C. Liu, N.P. Dasgupta, and P. Yang, *Chem. Mater.* 26, 1 (2014).
3. J.W. Ager, M.R. Shaner, K.A. Walczak, I.D. Sharp, and S. Ardo, *Energy Environ. Sci.* 8, 10 (2015).
4. M.G. Walter, E.L. Warren, J.R. McKone, S.W. Boettcher, Q. Mi, E.A. Santori, and N.S. Lewis, *Chem. Rev.* 110, 11 (2010).
5. S. Chen, S.S. Thind, and A. Chen, *Electrochem. Commun.* 63, 10–17 (2016).
6. N.P. Dasgupta and P. Yang, *Front. Phys.* 9, 3 (2014).
7. S. Hu, M.R. Shaner, J.A. Beardslee, M. Lichterman, B.S. Brunschwig, and N.S. Lewis, *Science* 344, 6187 (2014).
8. S. Hu, N.S. Lewis, J.W. Ager, J. Yang, J.R. McKone, and N.C. Strandwitz, *J. Phys. Chem. C* 119, 43 (2015).
9. M.F. Lichterman, K. Sun, S. Hu, X. Zhou, M.T. McDowell, M.R. Shaner, M.H. Richter, E.J. Crumlin, A.I. Carim, F.H. Saadi, B.S. Brunschwig, and N.S. Lewis, *Catal. Today* 262, 11–23 (2016).
10. F. Dimroth, *Phys. Status Solidi* 3, 3 (2006).
11. M. Bosi and C. Pelosi, *Prog. Photovoltaics Res. Appl.* 15, 1 (2007).
12. W. Shockley and H.J. Queisser, *J. Appl. Phys.* 32, 3 (1961).
13. S. Hu, C.-Y. Chi, K.T. Fountaine, M. Yao, H.A. Atwater, P.D. Dapkus, N.S. Lewis, and C. Zhou, *Energy Environ. Sci.* 6, 6 (2013).
14. L. Trotochaud, S.L. Young, J.K. Ranney, and S.W. Boettcher, *J. Am. Chem. Soc.* 136, 18 (2014).
15. K.L. Nardi, N. Yang, C.F. Dickens, A.L. Strickler, and S.F. Bent, *Adv. Energy Mater.* 5, 17 (2015).
16. K. Sun, M.T. McDowell, A.C. Nielander, S. Hu, M.R. Shaner, F. Yang, B.S. Brunschwig, and N.S. Lewis, *J. Phys. Chem. Lett.* 6, 4 (2015).
17. K. Sun, F.H. Saadi, M.F. Lichterman, W.G. Hale, H.-P. Wang, X. Zhou, N.T. Plymale, S.T. Omelchenko, J.-H. He, K.M. Papadantonakis, B.S. Brunschwig, and N.S. Lewis, *Proc. Natl. Acad. Sci. U.S.A.* 112, 12 (2015).
18. S.P. Mitoff, *J. Chem. Phys.* 35, 3 (1961).